Assessing 3D paediatric foot morphology using low-dose biplanar radiography: Parameter reproducibility and preliminary values

Virginie Rampal[a,b,*], Pierre-Yves Rohan[a], Rebekah Saksik[a], Philippe Wicart[c], Wafa Skalli[a]

[a] *Institut de Biomécanique Humaine Georges Charpak, Arts et Métiers ParisTech, 151, boulevard de l'hôpital, 75013 Paris, France*
[b] *Service d'orthopédie pédiatrique, hôpitaux pédiatriques de Nice CHU Lenval, 57, avenue de la Californie, 06000 Nice, France*
[c] *Service d'orthopédie pédiatrique, Hôpital Necker-Enfants Malades, 149, rue de Sèvres, 75015 Paris, France*

Keywords:

Foot
Stereoradiography
Reproducibility
Parameter values
Standing position
Paediatric patient

A B S T R A C T

Background: The physical examination and weight-bearing radiography are the two main available meth-ods for assessing the feet and lower limbs. The anatomy and function of these two structures interact with each other. These two assessment methods are affected by subjectivity and projection bias. Low-dose biplanar radiography (LDBR) is now a promising alternative for evaluating the lower limbs in children. At present, however, the foot cannot be assessed using LDBR. The objective of this study was to work towards developing a new method for 3D radiographic analysis of the paediatric foot during weight-bearing, first by determining the reproducibility of landmarks defined by LDBR then by reporting the values of the calculated radiographic parameters.
Hypothesis: A new radiographic method based on LDBR can be used to obtain a 3D evaluation of the foot in paediatric patients.
Patients and methods: Two biplanar radiographs in perpendicular planes were obtained simultaneously in a standardised position using the EOS system (EOS® Imaging, Paris, France) in each of 10 healthy children. To assess measurement uncertainty, two observers performed 3D reconstructions of each of the 10 feet three times (60 reconstructions). The standard error of reproducibility of the anatomic landmarks and clinical parameters was computed. Measurement uncertainty was then estimated based on the 95%confidence interval (95%CI). To obtain reference values, the mean ± SD of each variable was computed after checking that the data were normally distributed.
Results: Reproducibility was high for the anatomical landmarks of interest, calcaneal pitch angle, tibio-calcaneal angle on the lateral view, and first metatarsal pitch angle (95%CI < 5%). The values of these angles in the study population are reported.
Discussion and conclusion: The data reported here pave the way towards developing new parameters for describing 3D foot morphology and for simultaneously assessing the lower limb and foot in the standing position.
Level of evidence: I.

1. Introduction

Foot abnormalities affect both lower-limb position and gait. Their evaluation may be challenging, due to the absence of methods for assessing the entire lower limbs and feet in the standing position. The reliability of the physical examination varies with the experience of the examiner, and plain radiography, although far more accurate than the physical examination [1–4], is subjected to projection bias, particularly when deformities in the coronal plane are combined with deformities in the transverse or sagittal plane [5]. For instance, in patients with pes cavus, Meary's angle measured on the lateral radiograph is modified by adduction of the calcaneo-pedal unit or by rotation of the tibio-talo-fibular unit [6]. Challenges to the radiographic analysis in paediatric patients are related not only to the position of the foot on the ground, but also to the skeletal immaturity with incomplete ossification and variations across age groups. Other imaging techniques such as computed tomography and magnetic resonance imaging can also be used in everyday clinical practice but provide only

* Corresponding author. Institut de Biomécanique Humaine Georges Charpak, Arts et Métiers ParisTech, 151, boulevard de l'hôpital, 75013 Paris, France.
E-mail address: rocher-rampal.v@pediatrie-chulenval-nice.fr (V. Rampal).

https://doi.org/10.1016/j.otsr.2018.07.023

Fig. 1. Foot position during acquisition of the biplanar radiographs.

non-weight-bearing images, as the recently developed techniques for simulating weight-bearing are not yet widely available. Finally, these methods do not allow the simultaneous analysis of the lower limb and foot during weight-bearing [7].

Three-dimensional (3D) reconstruction from calibrated low-dose biplanar radiographs (LDBRs) is therefore of considerable interest. The LDBR technique has been validated for many anatomical regions [8–13] and holds promise compared to standard techniques [14,15]. Regarding the foot, a preliminary 3D reconstruction study in adults was published recently [16] and supports the possibility of objectively quantifying angles such as calcaneal pitch and lamina pedis twist [17]. However, models developed in adults are not suitable for use in children, as the incomplete ossification during the growth period hinders the identification of landmarks that are visible clearly in adults, thereby leading to poor reproducibility of 3D reconstructions.

The objective of this study was to work towards developing a new method for 3D radiographic analysis of the paediatric foot, first by determining the reproducibility of landmarks defined by LDBR then by reporting the values of the calculated radiographic parameters. The working hypothesis was that a new radiographic method based on LDBR can be used to obtain a 3D evaluation of the foot in paediatric patients.

2. Patients and methods

2.1. Patients

The study was approved by the local ethics committee (CPP 2013-A01568-37, n°° 76 09 2013). Ten healthy children, 6 girls and 4 boys ranging in age from 9 to 13 years, were included prospectively at the paediatric orthopaedics outpatient clinic where they were evaluated for minor lower-limb abnormalities that had no impact on the feet. None of the patients had symptoms in the feet, and the physical findings were considered normal by a senior orthopaedic surgeon specialised in the foot. Written informed consent was obtained from the patients and their parents.

For radiograph acquisition, the patients were positioned according to published recommendations [16] with the weight on the left foot and the toes of the right foot touching the surface (Fig. 1). Two calibrated LDBRs in perpendicular planes were acquired simultaneously in about 10 seconds using the EOS system (EOS Imaging, Paris,

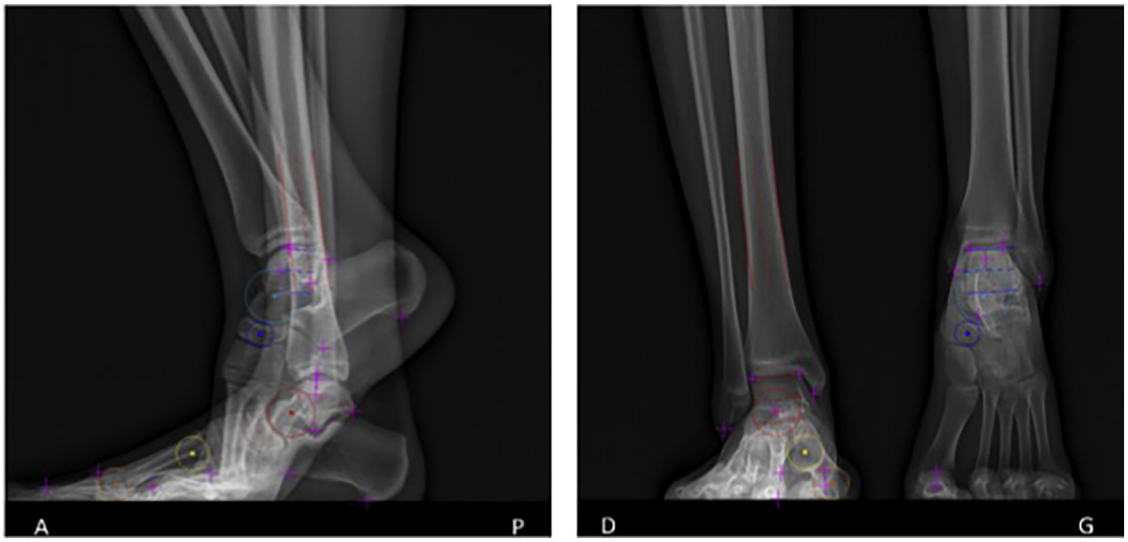

Fig. 2. Simplified parametric model: anatomical landmarks and geometric primitives.

Table 1
Anatomical landmarks on the lateral radiograph of the foot.

Bone	Name of the point	Anatomical landmark
Calcaneus	PC	Postero-inferior point of contact of the calcaneus with the ground
	AC	Most anterior point of the lower part of the calcaneus
Talus	SMT	Supero-medial angle of the talar dome
	SLT	Supero-lateral angle of the talar dome
	PT	Most posterior point of the talus
Hallux	HP1	Superior part of the base of the first phalanx of the great toe
Medial malleolus	MM	
Lateral malleolus	LM	

France). Exposure parameters were as follows: antero-posterior view, 60 kV, 200 mA, and 400 mGy/cm^2; and lateral view, 70 kV, 200 mA, and 500 mGy/cm^2.

2.2. Method

3D reconstructions of each foot were obtained using dedicated software developed at the *Institut de Biomécanique Humaine Georges Charpak*, Arts et Métiers ParisTech University, Paris (France), based on previously suggested methods [11,16]. The data were digitised then used to develop a simplified parametric model by representing the bones by eight landmarks and six stereo-corresponding geometric primitives (four spheres and two cylinders) defined on the antero-posterior and lateral views of each foot (Fig. 2, Tables 1 and 2). The simplified parametric model was then

Table 2
Geometric primitives selected to represent the talus, navicular bone, first metatarsal, and tibia.

Bone	Geometric primitives	Illustration
Talus	1 elliptical body cylinder (talar dome): EBC 1 sphere (talar head): TH	
Navicular bone	1 sphere: NB	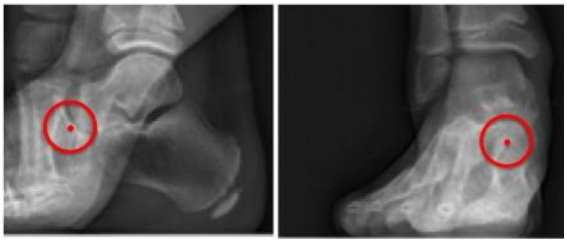
First metatarsal	2 spheres (head and base)	
Tibia	1 elliptical cylinder	

Fig. 3. A. Calcaneal pitch angle. B. Tibio-calcaneal angle. C. Talo-calcaneal divergence. D. Tibio-talar angle. E. Talo-navicular coverage angle. F. Méary's talo-metatarsal angle. G. Talo-metatarsal angle, dorso-plantar. H. First metatarsal pitch angle.

back-projected onto the antero-posterior and lateral radiographs. Adjustments were made manually to improve the match between the back-projected elements and the bone contours.

Radiographic parameters that are widely used in every day practice were chosen and programmed for automatic computation. To this end, some of the anatomical landmarks were simplified as follows:

- the tibia by a cylinder;
- the calcaneus by a line (PC-AC) from the postero-inferior point of contact of the calcaneus with the ground (PC) to the most anterior point of the lower part of the calcaneus (AC);
- the talar head by a sphere (TH) and the body by an elliptical cylinder (EBC);
- the navicular bone by a sphere (NB);

- the first metatarsal (M1) by two spheres, one proximal and one distal, whose centres defined the axis of M1;
- the calcaneal pitch angle between the ground and the PC-AC line (Fig. 3A);
- the tibio-calcaneal angle between the tibial shaft and the PC-AC line (Fig. 3B);
- the angle of talo-calcaneal divergence, between the PC-AC line and the axis of the EBC (Fig. 3C);
- the tibio-talar angle between the tibial shaft and the axis of the EBC (Fig. 3D);
- the talo-navicular coverage angle (Fig. 3E) between the axis of the EBC and the line connecting the centres of NB and TH;
- Meary's angle between the axis of M1 and the axis of the EBC (Fig. 3F);
- the talo-metatarsal angle on the antero-posterior view (Fig. 3G);
- the pitch angle of M1 between the ground and the axis of M1 (Fig. 3H).

2.3. Assessment methods

For the evaluation of measurement uncertainty, two observers, an orthopaedic surgeon and an engineer, both experts in foot anatomy and reconstruction methods, each performed the 3D reconstructions of the 10 feet three times, yielding 60 reconstructions. At least 1 day was allowed to elapse between two reconstructions of the same foot.

2.4. Statistical analysis

The inter-observer reproducibility standard deviation (SD_r) was computed using the method described in the ISO standard 5725. Reproducibility was then estimated by computing the 95% confidence interval (95%CI) (=2·SD_r). We considered that 95%CI results consistent with use in clinical practice were less than 6 mm for the positions of the anatomical landmarks and geometric primitives and less than 5° for the radiographic parameters.

To establish reference values, we checked data distribution normality then computed the mean ± SD of each parameter.

3. Results

Table 3 reports the measurement uncertainties for the anatomical landmarks and geometric primitives. Except for AC on the Y-axis, the SD_r was consistently less than 3 mm (95%CI < 6 mm). Orientation of the axis of the tibial cylinder had an SD_r < 1° (95%CI < 2°) and orientation of the axis of the EBC an SD_r < 3° (95%CI < 6°).

Among radiographic parameters, the most reliable were the tibio-calcaneal angle on the lateral view, the calcaneal pitch angle, the M1 pitch angle, and the tibio-talar angle on the antero-posterior view (95%CI < 5°). The 95%CI was greater than 5% for the talo-calcaneal angle, talo-navicular coverage angle, Méary's angle, and talo-metatarsal angle on the antero-posterior view (Table 4).

The values of the radiographic parameters computed from the 3D reconstructions of the 10 feet were normally distributed. Table 5 reports the mean value and inter-individual SD for the tibio-calcaneal angle on the lateral view, calcaneal pitch angle, M1 pitch angle, and tibio-talar angle on the antero-posterior view.

Table 3
95% confidence intervals (95%CIs, 2SDs) for the anatomical landmarks and geometric primitives (in millimetres).

	x	y	z
Calcaneus			
Most anterior point of the lower part	5	11	4
Postero-inferior point of contact of the calcaneus with the ground	6	8	2
Hallux			
First phalanx	4	4	4
Malleolus			
Lateral	5	2	2
Medial	5	2	2
Talus			
Supero-lateral point	4	2	2
Supero-medial point	3	2	2
Posterior point	3	4	4
Navicular bone	4	5	3
Talar head	5	3	3
First metatarsal			
Proximal part	5	5	4
Distal part	4	5	3

Table 4
95% confidence intervals (95%CIs, 2SDs) for the radiographic parameters (in degrees).

	95%CI 2D value	95%CI 3D value
Calcaneal pitch angle	5	6
Tibio-calcaneal angle (lateral)	5	5
Tibio-talar angle (antero-posterior)	5	5
Talo-calcaneal angle	15	17
Talo-navicular coverage angle	19	15
Méary's angle	13	14
Angle between the talus and first metatarsal (antero-posterior)	17	14
First metatarsal pitch angle	5	5

4. Discussion

The study results confirm the working hypothesis by showing that the tibio-calcaneal angle, calcaneal pitch angle, M1 pitch angle, and antero-posterior tibio-talar angle are highly reproducible (SD_r = 2.5°, 95%CI < 5%). These findings are consistent with data obtained using standard radiographs [18]. Reproducibility was less good for the parameters involving the calcaneus, as bony superimpositions made the AC point difficult to identify on the antero-posterior view (Fig. 4A). When following the X-axis on the lateral view, the PC point was sometimes challenging to identify, depending on the degree of ossification, which varied widely across patients (Fig. 4B).

Although 3D reconstruction techniques based on calibrated LDBRs hold promise for analysing the musculo-skeletal system in everyday clinical practice, a single preliminary study of 3D reconstructions of the foot and ankle in adults is available [16], and the data needed to apply this technique to the paediatric foot are not

Table 5
Values of the radiographic parameters (in degrees) and comparison with previously published values.

	2D	3D	Mean (range)	Bourdet et al.,[17]	Davids et al., [18]	Steel et al., [19]	Moraleda et al., [20]
Number of feet	10			65	60		135
Age (years)	9–13			7–18	5–17	Adults	Adults
Tibio-calcaneal angle (lateral)	67°	67°	54° 77°		65° 75°		61° 83°
Calcaneal pitch angle	20°	18°	14° 34°	20° 30°	5° 32°	11° 38°	11° 23°
Tibio-talar angle (antero-posterior)	0°	0°	−10° 7°		−9° 12°		
First metatarsal pitch angle	21°	20°	15° 30°	10° 20°	1° 13°	16° 30°	

Fig. 4. A. Calcanei, coronal view: point AC cannot be identified on this view. B. Calcaneum, lateral view: point PC is difficult to identify due to the insufficient ossification.

available. The objectives of this study were to evaluate the reliability of radiographic 3D reconstructions of the paediatric foot in the functional weight-bearing position and to report the values of radiographic parameters in the study population. In clinical practice, a radiological evaluation is indispensable to establish the diagnosis (by comparison with normal ranges), for the longitudinal follow-up, and to analyse changes in an abnormality. In every case, the evaluation of measurement uncertainty (95%CI) confirmed the clinical relevance of the measurements performed for the study.

This work obtained values for a limited number of radiographic parameters, particularly in comparison to a recent study in adults [16]. Two factors explain this difference. First, in children, reproducible anatomical landmarks are difficult to define because the degree of ossification changes with age, thus continuously modifying the landmarks. Second, the smaller size of the paediatric foot increases the risk of major angle measurement uncertainty. Nevertheless, the radiographic parameters chosen for our study are indispensable to paediatric orthopaedic surgeons for analysing the foot [17–20] (Table 5). Several angles must be measured in combination, since a comprehensive description of foot anatomy combines descriptions of the hindfoot, midfoot, and forefoot [18,19,21]. The values of the parameters found in our study are consistent with the reported normal ranges of the same parameters measured on 2D radiographs and can therefore be used by clinicians. Here, the difference between 2D measurements and computed 3D angles was minimal (Table 5). However, this tiny difference was found for normal feet. In patients with disorders of the foot, the bone and joint abnormalities increase the alteration of 2D measurements by projection bias.

This study has two main limitations. First, only 10 feet were included. A larger sample size would have increased the statistical power of the analysis and provided reference values. However, a sample size of 10 was sufficient to assess reproducibility and to obtain preliminary results. The second limitation is that we studied

only reproducibility and not accuracy. To assess accuracy, the angle values calculated using our method would have to be compared to those obtained using 1 mm-thick computed tomography slices, which would raise ethical problems related to the radiation dose to which the children would be exposed.

In conclusion, our findings confirm the usefulness of LDBRs for describing the paediatric foot. The 3D radiographic landmarks and associated parameters are reliable and reproducible. To our knowledge, no method is available for obtaining a 3D assessment of the paediatric foot during weight-bearing. This preliminary study describes a rapid method for improving the assessment of relationships among bones in the functional position. It paves the way for developing new parameters for a 3D description of the paediatric foot and for simultaneously investigating the foot and lower limb in the standing position.

Disclosure of interest

Wafa Skalli is the co-inventor of the EOS system but derives no personal financial benefit from this fact.

The authors declare that they have no competing interest.

Funding

None.

Contributions of each author

V. Rampal included the patients, designed the study, performed the reconstructions, and wrote the manuscript.

P.Y. Rohan performed the statistical analysis, was in charge of the computations and informatics programme, and revised and corrected the manuscript.

R. Saksik developed the reconstruction programme.

P. Wicart designed and supervised the study and revised the manuscript.

W. Skalli designed and supervised the study and revised the manuscript.

Acknowledgements

We thank the *Programme de Chaire ParisTech BiomecAM* for help with the musculo-skeletal modelling project and Thomas Joubert for technical assistance.

References

[1] Fabry G, Clinical practice. Static, axial, and rotational deformities of the lower extremities in children. Eur J Pediatr 2010;169:529–34.

[2] Heath CH, Staheli LT. Normal limits of knee angle in white children–genu varum and genu valgum. J Pediatr Orthop 1993;13:259–62.

[3] Hinman RS, May RL, Crossley KM. Is there an alternative to the full-leg radiograph for determining knee joint alignment in osteoarthritis? Arthritis Rheum 2006;55:306–13.

[4] Kraus VB, Vail TP, Worrell T, McDaniel G. A comparative assessment of alignment angle of the knee by radiographic and physical examination methods. Arthritis Rheum 2005;52:1730–5.

[5] Gheno R, Nectoux E, Herbaux B, Baldisserotto M, Glock L, Cotten A, et al. Three-dimensional measurements of the lower extremity in children and adolescents using a low-dose biplanar X-ray device. Eur Radiol 2012;22:765–71.

[6] Seringe R, Wicart P. French Society of Pediatric Orthopaedics. The talonavicular and subtalar joints: the "calcaneopedal unit" concept. Orthop Traumatol Surg Res 2013;99:S345–55.

[7] Ledoux WR, Rohr ES, Ching RP, Sangeorzan BJ. Effect of foot shape on 3-dimensional position of foot bones. J Orthop Res 2006;24:2176–86.

[8] Pomero V, Mitton D, Laporte S, de Guise JA, Skalli W. Fast accurate stereoradiographic 3D-reconstruction of the spine using a combined geometric and statistic model. Clin Biomech 2004;19:240–7.

[9] Sabourin M, Jolivet E, Miladi L, Wicart P, Rampal V, Skalli W. Three-dimensional stereoradiographic modeling of the rib cage before and after spinal growing rod procedures in early onset scoliosis. Clin Biomech (Bristol, Avon) 2010;25:284–91.

[10] Lebailly F, Lima LV, Clairemidi A, Aubert B, Guerard S, Chaibi Y, et al. Semi-automated stereoradiographic upper limb 3D reconstructions using a combined parametric and statistical model: a preliminary study. Surg Radiol Anat 2011;34:757–65.

[11] Chaibi Y, Cresson T, Aubert B, Hausselle J, Neyret P, Hauger O, et al. Fast 3D reconstruction of the lower limb using a parametric model and statistical inferences and clinical measurements calculation from biplanar X-rays. Comput Methods Biomech Biomed Engin 2012;15:457–66.

[12] Quijano S, Serrurier A, Aubert B, Laporte S, Thoreux P, Skalli W. Three-dimensional reconstruction of the lower limb from biplanar calibrated radiographs. Med Eng Phys 2013;35:1703–12.

[13] Rampal V, Rohan PY, Assi A, Ghanem I, Rosello O, Simon AL, et al. Lower-limb lengths and angles in children older than 6 years: reliability and reference values by EOS stereoradiography. Orthop Traumatol Surg Res 2018;104:389–95.

[14] Gaumétou E, Quijano S, Ilharreborde, Presedo A, Thoreux P, Mazda K, et al. EOS® analysis of lower extremity segmental torsion in children and young adults. Orthop Traumatol Surg Res 2014;100:147–51.

[15] Meyrignac O, Moreno R, Baunin C, Vial J, Accadbled F, Sommet A, et al. Low-dose biplanar radiography can be used in children and adolescents to accurately assess femoral and tibial torsion and greatly reduce irradiation. Eur Radiol 2015;25:1752–60.

[16] Rohan PY, Perrier A, Ramanoudjame M, Hausselle J, Lelièvre H, Seringe R, et al. 3D reconstruction of foot in the weight-bearing position from bi-planar X-ray radiographs: evaluation of accuracy and reliability. J Foot Ankle Surg 2018, http://dx.doi.org/10.1053/j.jfas.2018.03.014 [Epub ahead of print].

[17] Bourdet C, Seringe R, Adamsbaum C, Glorion C, Wicart P. Flatfoot in children and adolescents. Analysis of imaging findings and therapeutic implications. Orthop Traumatol Surg Res 2013;99:80–7.

[18] Davids JR, Gibson TW, Pugh LI. Quantitative segmental analysis of weight-bearing radiographs of the foot and ankle for children: normal alignment. J Pediatr Orthop 2005;25:769–76.

[19] Steel MW, Johnson KA, DeWitz MA, Ilstrup DM. Radiographic measurements of the normal adult foot. Foot Ankle 1980;1:151–8.

[20] Moraleda L, Mubarak SJ. Flexible flatfoot: differences in the relative alignment of each segment of the foot between symptomatic and asymptomatic patients. J Pediatr Orthop 2011;31:421–8.

[21] Roth S, Roth A, Jotanovic Z, Madarevic T. Navicular index for differentiation of flatfoot from normal foot. Int Orthop 2013;37:1107–12.